Emergent Kondo Lattice Behavior in Iron-Based Superconductors AFe_2As_2 (A = K, Rb, Cs)

Y. P. Wu,[1] D. Zhao,[1] A. F. Wang,[1] N. Z. Wang,[1] Z. J. Xiang,[1] X. G. Luo,[1,2,3] T. Wu,[1,2,3,*] and X. H. Chen[1,2,3,4,†]
[1]Hefei National Laboratory for Physical Science at Microscale and Department of Physics, University of Science and Technology of China, Hefei, Anhui 230026, China
[2]Key Laboratory of Strongly Coupled Quantum Matter Physics, University of Science and Technology of China, Chinese Academy of Sciences, Hefei 230026, China
[3]Collaborative Innovation Center of Advanced Microstructures, Nanjing University, Nanjing 210093, China
[4]High Magnetic Field Laboratory, Chinese Academy of Sciences, Hefei, Anhui 230031, China
(Received 14 December 2015; published 7 April 2016)

Here, we experimentally study the origin of d-electron heavy fermion (HF) behavior in iron-based superconductors (FeSCs) AFe_2As_2 (A = K, Rb, Cs). Nuclear magnetic resonance on ^{75}As reveals a universal coherent-incoherent crossover with a characteristic temperature T^*. Below T^*, a so-called "Knight shift anomaly" is first observed in FeSCs, which exhibits a scaling behavior similar to f-electron HF materials. Furthermore, the scaling rule also regulates the manifestation of magnetic fluctuation. These results undoubtedly support an emergent Kondo lattice scenario for the d-electron HF behavior, which qualifies the AFe_2As_2 (A = K, Rb, Cs) as d-electron HF superconductors.

DOI: 10.1103/PhysRevLett.116.147001

Superconductivity in heavy fermion (HF) materials is a conundrum in condensed matter physics. The conventional phonon-mediated pairing mechanism fails in this case, suggesting an unconventional pairing mechanism similar to that in cuprates and organic superconductors [1]. The Kondo lattice model has been widely accepted as the starting point for discussing the underlying physics [2–5]. Although the Kondo lattice picture for HF has achieved a great success in f-electron materials, the fate of the Kondo lattice picture in HF materials without f electrons, especially for d-electron systems, is still controversial [6–9]. Furthermore, whether similar HF superconductivity as f-electron systems could be achieved in d-electron materials is still under debate.

Recently, a remarkable mass enhancement was observed in heavily hole-doped Fe-based superconductors (FeSCs) AFe_2As_2 (A = K, Rb, Cs). As shown in Fig. 1, an apparent particle-hole asymmetry for effective mass (m^*) appears in doped $BaFe_2As_2$ [10–13]. In heavily hole-doped KFe_2As_2, the value of the Sommerfeld coefficient (γ) has reached 98 m J mol K^2 [10]. Quantum oscillation and angle-resolved photoemission spectroscopy (ARPES) experiments also support the mass enhancement [14,15]. Furthermore, the m^* becomes even heavier by replacing K^+ by larger alkaline ions of Rb^+ ($\gamma \sim 127$ mJ mol K^2) [12] and Cs^+ ($\gamma \sim 184$ mJ mol K^2) [12]. In FeSCs, the Hund's coupling is highly important for the correlation effect instead of on-site Coulomb interaction [16], which has a strong effect on band renormalization in FeSCs [17]. However, recent theoretical calculation suggests that the remarkable mass enhancement in AFe_2As_2 (A = K, Rb, Cs) is beyond naive band renormalization [18]. On the other hand, a coexistence of itinerant and local characters for $3d$ electrons has been widely recognized as an elementary feature in FeSCs [19], which hints at a possible Kondo scenario for the mass enhancement in AFe_2As_2 (A = K, Rb, Cs). In fact, a coherent-incoherent crossover similar to f-electron HF has already been proposed for FeSCs [16], which is recalled by recent bulk magnetic susceptibility and thermal expansion experiments on KFe_2As_2 [20]. However, there is still no consensus on the Kondo picture experimentally. Here, we systematically perform ^{75}As nuclear magnetic resonance (NMR) experiments to study the hole-doped FeSCs AFe_2As_2 (A = K, Rb, Cs). Our results

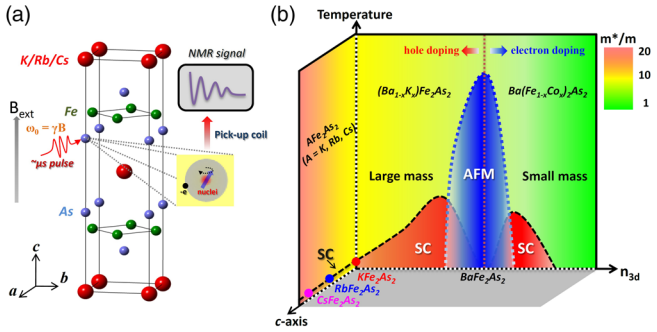

FIG. 1. (a) Crystal structure of heavily hole-doped FeSCs AFe_2As_2 (A = K, Rb, Cs) and sketch of NMR experiment. The local symmetry of the As site is tetragonal with four nearest-neighbor Fe atoms. We performed NMR measurements on ^{75}As nuclei. (b) Schematic phase diagram of FeSCs with 122 structure tuned by the number of $3d$ electrons (n_{3d}) at Fe sites. The color in the phase diagram depicts effective the mass m^* relative to that from band theory. SC denotes superconducting phase. AFM denotes antiferromagnetic phase.

strongly support the Kondo scenario for HF in AFe_2As_2 (A = K, Rb, Cs) and qualifies AFe_2As_2 (A = K, Rb, Cs) as d-electron HF superconductors under the frame of the Kondo lattice scenario.

In Fig. 2, one of the main findings in the present Letter is a universal electronic crossover observed in both the temperature-dependent Knight shift (K) and resistivity in AFe_2As_2 (A = K, Rb, Cs). In general, $K = K_{orb} + K_s$, where K_{orb} is the orbital contribution and K_s is the spin contribution. K_s is usually temperature-dependent, while K_{orb} is always temperature-independent in FeSCs. K_s is proportional to local spin susceptibility (χ_{loc}) at the nearest-neighbor Fe atoms through the transferred hyperfine coupling tensor ($K_s = A\chi_{loc}$). In a uniform paramagnetic state, since χ_{loc} is proportional to χ_{bulk}, K_s must be scaled with bulk magnetic susceptibility (χ_{bulk}). Therefore, the temperature-dependent Knight shift could be expressed as $K(T) = A\chi_{bulk}(T) + K_{orb}$. As shown in Fig. 2, the temperature-dependent part of the Knight shift above T^* is consistent with a Curie-Weiss behavior for all samples, suggesting a local-moments dominated behavior. Similar behavior has also been confirmed in bulk magnetic susceptibility measurements (See Supplemental Material [21]). As the temperature decreases below T^*, the Knight shift undergoes a crossover to deviate from the high-temperature Curie-Weiss behavior. There is a roughly 10% decrease in the values of the Knight shift for all samples. Finally, the temperature-dependent Knight shift becomes saturated at low temperature. The T^* for AFe_2As_2 (A = K, Rb, Cs) shows a continuous suppression with

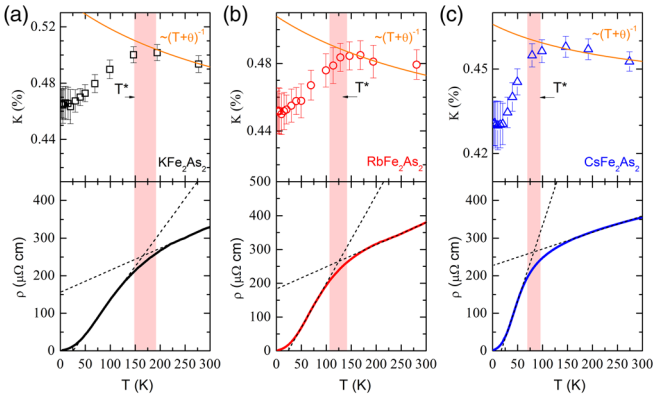

FIG. 2. Top panels: Temperature-dependent Knight shift (K) for (a) KFe_2As_2; (b) $RbFe_2As_2$; (c) $CsFe_2As_2$. External magnetic field (B_{ext}) was applied parallel to the c axis with a magnitude of 12 Tesla. Solid lines represent simulated Curie-Weiss behavior to fit $K(T)$ above T^*. The values of θ are determined from the Curie-Weiss fitting on the corresponding bulk magnetic susceptibility (See Supplemental Material [21]). Bottom panels: Temperature-dependent resistivities for (a) KFe_2As_2; (b) $RbFe_2As_2$; (c) $CsFe_2As_2$. The dashed lines are two tentative T-linear trends to extract the value of T^* from resistivity. The bold pink lines mark nearly the same T^* determined by Knight shift and resistivity.

replacing K^+ ($T^* \sim 165 \pm 25$ K) with larger alkaline ions of Rb^+ ($T^* \sim 125 \pm 20$ K) and Cs^+ ($T^* \sim 85 \pm 15$ K). Although the broad linewidth made the crossover behavior indistinguishable in the Knight shift in earlier experiments on KFe_2As_2 [28], bulk magnetic susceptibility and thermal expansion experiments showed a similar crossover behavior in KFe_2As_2 [20], consistent with the present NMR results. Surprisingly, the T^* (~100 K) determined by the maximum of χ_{bulk} is much lower than that determined from the Knight shift measurement ($T^* \sim 165 \pm 25$ K). Besides KFe_2As_2, a similar discrepancy of T^* is also observed for $RbFe_2As_2$ and $CsFe_2As_2$. The impurity effect might be a reason for this discrepancy. In fact, a clear Curie-Weiss tail due to the impurity effect is observed in the bulk magnetic susceptibility (See Supplemental Material [21]), while it is absent in the Knight shift. A possible explanation for this difference is that NMR is a local probe for spin susceptibility and trivial impurities do not affect the Knight shift measured by ^{75}As nuclei away from impurities. However, even if we try to subtract the Curie-Weiss tail from χ_{bulk}, the discrepancy for T^* is not improved at all (See Supplemental Material [21]). It suggests an intrinsic "Knight shift anomaly" which will be further discussed in the following pages.

On the other hand, a similar electronic crossover behavior also appears in charge transport as shown in Fig. 2. Temperature-dependent resistivity shows a crossover behavior at T^*. Below T^*, the positive slope of resistivities for all samples shows a significant change. We try to use the cross point of two T-linear trends to determine T^* in resistivity. It is evident that both the temperature-dependent Knight shift and resistivity have a consistent crossover behavior at nearly the same T^*. We would like to emphasize that such similar crossover behavior in both the Knight shift and resistivity has been widely observed in f-electron HF materials [4,29]. The great similarity to f-electron materials strongly suggests a possible Kondo scenario for AFe_2As_2 (A = K, Rb, Cs). Indeed, such a coherent-incoherent crossover for $3d$ electrons has already been proposed in theory for FeSCs [16,17], and our work clearly manifests such a case. However, these results are still not enough to settle the microscopic origin of d-electron HF behavior in AFe_2As_2 (A = K, Rb, Cs), especially for the Kondo lattice scenario.

In order to further understand the microscopic origin of d-electron HF behavior, we explore the possible Kondo scaling behavior in AFe_2As_2 (A = K, Rb, Cs). As we mentioned, an intrinsic Knight shift anomaly is revealed by comparing the temperature-dependent Knight shift and bulk magnetic susceptibility. In Fig. 3(a), the $K - \chi_{bulk}$ plot for all samples shows a clear deviation from linear behavior around T^*. It suggests that the Knight shift is no longer scaled with bulk magnetic susceptibility below T^*. A similar phenomenon has been widely found in f-electron HF materials [29]. In a so-called two-fluid model of heavy

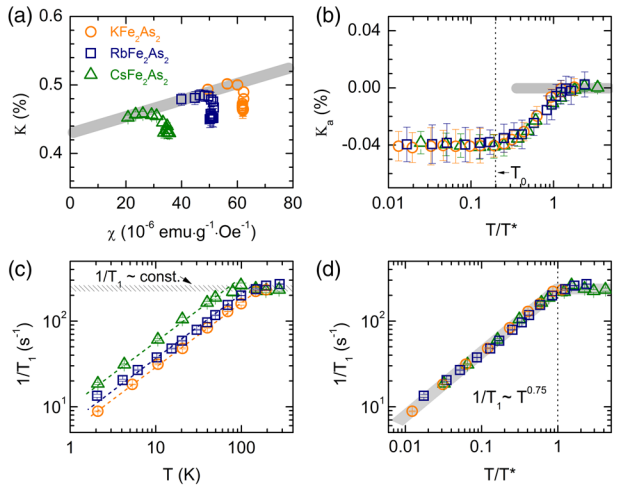

FIG. 3. (a) $K-\chi$ plot for AFe_2As_2 (A = K, Rb, Cs). The Knight shift data used here are the same as that in Fig. 2. The grey bold line is a guide for eyes. It points out a clear deviation from linear behavior around T^*. Here, the Curie-Weiss tail contribution on bulk magnetic susceptibility (χ) has already been subtracted (See Supplemental Material [21]). Although there is some unavoidable error for determined bulk magnetic susceptibility from estimation on the Curie-Weiss tail, this would not change the main conclusion in the present Letter. (b) Scaling behavior for the anomalous Knight shift (K_a). The definition of K_a is described in the main text. The dotted line represents another characteristic temperature T_0, below which the anomalous Knight shift becomes saturated. Here, T_0 is about $0.2T^*$. (c) Temperature-dependent $1/T_1$ for AFe_2As_2 family (A = K, Rb, Cs). The experimental details for $1/T_1$, see Supplemental Material [21]. Above T^*, $1/T_1$ exhibits a temperature independent behavior. Below T^*, all samples exhibit a similar temperature dependence with $1/T_1 \sim T^{0.75}$. (d) Scaling behavior for temperature-dependent $1/T_1$ in AFe_2As_2 (A = K, Rb, Cs). The grey bold line represents a universal scaling behavior with $1/T_1 \sim (T/T^*)^{0.75}$.

fermions [30,31], the Knight shift anomaly is ascribed to the coexistence of an itinerant Kondo liquid (KL) and local spin liquid (SL). The total bulk magnetic susceptibility could be expressed as $\chi = f(T)\chi_{\mathrm{KL}} + [1-f(T)]\chi_{\mathrm{SL}}$, where $f(T)$ is an order parameter to characterize the emergent KL component. The corresponding Knight shift is $K = K_0 + Af(T)\chi_{\mathrm{KL}} + B[1-f(T)]\chi_{\mathrm{SL}}$, in which the spin liquid component is coupled to the probe nucleus by a transferred hyperfine coupling constant B, while the itinerant KL component is coupled by a direct hyperfine coupling A. K_0 is a constant offset from orbital contribution. Then, the emergent anomalous part of the Knight shift is $K_a = K - K_0 - B\chi = (A-B)f(T)\chi_{\mathrm{KL}}$, which is proportional to χ_{KL} and shows a universal T^* scaling behavior in f-electron HF materials. In the current case, we also adopt the two-fluid model to analyze the Knight shift anomaly. In Fig. 3(b), the extracted K_a for AFe_2As_2 (A = K, Rb, Cs) shows a perfect T^* scaling behavior similar to the f-electron HF systems. In f-electron HF systems, $f(T) \sim (1-T/T^*)^{3/2}$ and $\chi_{\mathrm{KL}} \sim 1 + \ln(T^*/T)$. The corresponding scaling behavior of K_a is proportional to $(1-T/T^*)^{3/2}[1+\ln(T^*/T)]$. It shows a divergent behavior as $T \to 0$, which is regulated by the divergence in the Sommerfeld coefficient ($\gamma \sim \chi_{\mathrm{KL}}$). For AFe_2As_2 (A = K, Rb, Cs), the scaling curve shows a saturation behavior below a characteristic temperature T_0 instead of divergent behavior as $T \to 0$. Since specific heat measurement for AFe_2As_2 (A = K, Rb, Cs) shows a temperature-independent Sommerfeld coefficient at low temperature (See Supplemental Material [21]), the saturation of K_a indicates that $f(T)$ reaches an upper limit and becomes constant below T_0. These results imply that the KL component in the two-fluid description is completely dominated, while the local spin liquid component disappears below T_0. Similar saturation behavior is also observed in f-electron HF materials, e.g., $CeSn_3$ and URu_2Si_2 [30,31]. In this case, a Landau Fermi-liquid behavior would emerge at lower temperature as expected in the two-fluid model [5]. This is also consistent with the previous observation of a T^2 behavior in charge transport, a temperature-independent Sommerfeld coefficient, and a Wilson ratio close to unity at low temperature [20]. Therefore, these observations strongly support a consistent Kondo lattice scenario under the two-fluid model.

In addition, we also studied the low-energy magnetic fluctuation for AFe_2As_2 (A = K, Rb, Cs). As shown in Fig. 3(c), we measured the temperature-dependent spin-lattice relaxation rate ($1/T_1$) which is related to the dynamical magnetic susceptibility $\mathrm{Im}\chi_\perp(q,\omega_n)$ with $1/T_1 = 2\gamma_n^2 T\sum_q A_\perp^2(q)\mathrm{Im}\chi_\perp(q,\omega_n)/\omega_n$, where $A_\perp(q)$ is the transferred hyperfine coupling tensor perpendicular to the external field direction at ^{75}As sites and $\omega_n = \gamma_n H$ is the NMR frequency. Usually, $1/T_1$ in the Landau Fermi-liquid state follows a Korringa-type behavior with $1/T_1T \sim N^2(E_F)$, where $N(E_F)$ is the density of state at the Fermi level and is temperature-independent. If local moments dominate the low-energy magnetic fluctuation, $1/T_1$ would obey a Curie-type behavior with $1/T_1T \sim T^{-1}$. In Fig. 3(c), the temperature-dependent $1/T_1$ for AFe_2As_2 (A = K, Rb, Cs) exhibits a similar crossover behavior at T^* to the Knight shift and resistivity shown in Fig. 2. Above T^*, $1/T_1$ shows a temperature-independent behavior, suggesting a local-moments dominated behavior. With decreasing temperature below T^*, a well-defined power-law behavior emerges with $1/T_1 \sim T^{0.75}$. Similar crossover behavior in $1/T_1$ has been observed in f-electron HF materials [4], in which the power index is different and strongly dependent on the type of quantum criticality nearby, such as 0 for $YbRh_2Si_2$ [32], 0.25 for $CeCoIn_5$ [33], and 1 for URu_2Si_2 [34]. The observed $T^{0.75}$ power-law behavior in AFe_2As_2 (A = K, Rb, Cs) might be ascribed to a specific quantum criticality, but it is still not very clear at the present stage [18,35], which needs further investigation. In Fig. 3(d), we also plot $1/T_1$ as a function of the renormalized temperature (T/T^*) for

AFe_2As_2 (A = K, Rb, Cs), and a universal scaling behavior for $1/T_1$ is observed. It suggests that the same scaling rule in the Knight shift anomaly also dominates the low-energy magnetic fluctuation below T^*. By T^* scaling, we can extract a universal $1/T_1$ formula in the coherent state, $1/T_1 = C(T/T^*)^{0.75}$, where $C = 238 \pm 2\ \mathrm{s}^{-1}$.

A recent high-resolution ARPES experiment has observed a temperature-dependent hybridization gap between d_{xy} and d_{xz} bands in iron chalcogenide superconductors [36]. Meanwhile, a considerable band renormalization effect was also revealed for the d_{xy} band. This result might be treated as a possible microscopic picture for the Kondo lattice scenario proposed in the present Letter. The d_{xy} band would play the role of local moments as f-electrons did in HF materials. The first principle calculation also supports the local character for the d_{xy} band in KFe_2As_2 [20], which is consistent with quantum oscillation [14] and the ARPES experiment [15]. Further high-resolution ARPES experiments to explore the hybridization gap and Kondo coherent peak would be required to complete the microscopic picture for the Kondo lattice scenario in AFe_2As_2 (A = K, Rb, Cs).

In various f-electron HF superconductors, the T_c is always less than the order of $0.1T^*$ [37]. In Fig. 4, we show a summary plot for the relationship among T_c, T^*, and γ. Although an empirical limitation of T_c is set to $0.1T^*$, it's very clear that higher T^* favors higher T_c. In Kondo lattice systems, T^* follows an empirical scaling behavior with $T^* = cJ^2\rho$ [4], in which J is the local Kondo coupling, and ρ is the density of states of the conduction electrons coupled to the local spins and c is a constant determined by the details of the hybridization and the conduction electron Fermi surface. The relationship between T_c and T^* (in Fig. 4) suggests that the unconventional superconductivity in HF superconductors is correlated to local magnetic coupling [37]. Based on the present NMR results, it's reasonable to classify the AFe_2As_2 family (A = K, Rb, Cs) as new HF superconductors without f electrons. As expected under the Kondo lattice scenario, the AFe_2As_2 family (A = K, Rb, Cs) exhibits a consistent tendency with the f-electron HF superconductors as shown in Fig. 4. The systematic evolution of local magnetic coupling due to modification of Fe-Fe distance by the alkali metal with a different ionic radius might be responsible for the variation of T^* in AFe_2As_2 family (A = K, Rb, Cs) [35]. On the other hand, T^* is also expected to be related to the Sommerfeld coefficient with $\gamma^{-1} \sim T^*$ in the two-fluid model of heavy fermions as the KL component becomes dominated at low temperature [5]. As shown in Fig. 3(b), the observed KL component in AFe_2As_2 family (A = K, Rb, Cs) also becomes dominated below T_0. Therefore, we would expect that the Sommerfeld coefficients at low temperature should be correlated to T^*. As shown in Fig. 4, the Sommerfeld coefficients of AFe_2As_2 family (A = K, Rb, Cs) do follow the same T^* dependent behavior as the f-electron HF

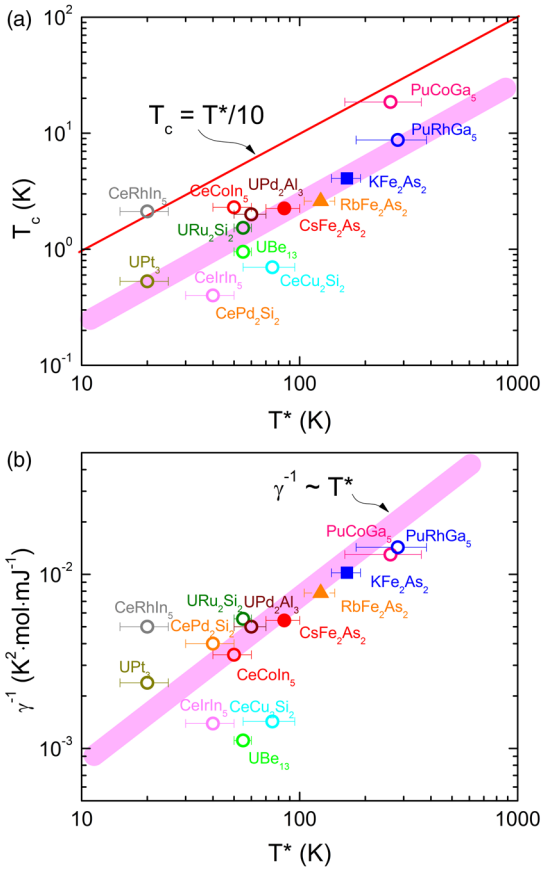

FIG. 4. (a) The correlation between the superconducting temperature T_c and the characteristic Kondo temperature T^* for f-electron HF superconductors and AFe_2As_2 (A = K, Rb, Cs). The red line is an empirical upper limit for the maximum of T_c for f-electron HF superconductors with a given T^*. The grey bold line is a guide for the eyes. It represents a universal tendency for the evolution of T_c with T^*. (b) The correlation between the Sommerfeld coefficient (γ) and T^* for f-electron HF superconductors and AFe_2As_2 (A = K, Rb, Cs). The grey bold line represents a universal relationship with $\gamma^{-1} \sim T^*$. It's clear that the reciprocal of the Sommerfeld coefficient in AFe_2As_2 (A = K, Rb, Cs) follows the grey bold line for most of f-electron HF superconductors. All data used in Fig. 4 are listed in the Supplemental Material [21].

superconductors. All these results further qualify AFe_2As_2 family (A = K, Rb, Cs) as d-electron HF superconductors under the frame of the Kondo lattice scenario.

In FeSCs, whether the pairing mechanism is from a weak coupling or strong coupling scenario has been intensively discussed in the past several years. To date, neither the weak coupling approach based on itinerant electrons, nor the strong coupling approach based on local moments is sufficient to account for all existing experimental results [19]. Both the itinerant electrons and local moments should be taken into account, which is somehow similar to the situations in heavy fermions. However, the physics for the involvement of itinerant electrons and local moments is, so far, still not clear. Our present findings shed new light on

this issue and clarify the underlying Kondo lattice physics. It would definitely improve our understanding of iron-based superconductors. On the other hand, as suggested by Fig. 4(a), an empirical route to understanding high-T_c superconductivity in the frame of HF physics is that high T^* favors high T_c [37], which also offers a way to search high-T_c superconductors. Here, in d-electron HF materials, the T^* would be expected to be higher than that of f-electron HF materials due to the stronger hybridization effect. Whether the newly discovered high-T_c superconductivity in FeSCs could be understood in this way would be an interesting issue. This would be helpful for building a universal picture of unconventional superconductivity in both FeSCs and HF superconductors.

The authors are grateful for the stimulating discussions with Z. P. Yin, G. Kotliar, Y.-F. Yang, G. M. Zhang, D. H. Lee, F. C. Zhang, M.-H. Julien, S. Y. Li, and Z. Sun. This work is supported by the National Natural Science Foundation of China (Grants No. 11190021, No. 11374281, No. 11522434), the "Strategic Priority Research Program (B)" of the Chinese Academy of Sciences (Grant No. XDB04040100), the National Basic Research Program of China (973 Program, Grant No. 2012CB922002), the Fundamental Research Funds for the Central Universities and the Chinese Academy of Sciences. T. W. acknowledges the Recruitment Program of Global Experts and the CAS Hundred Talent Program.

*wutao@ustc.edu.cn
†chenxh@ustc.edu.cn

[1] P. Monthoux, D. Pines, and G. G. Lonzarich, Nature (London) **450**, 1177 (2007).
[2] P. Gegenwart, Q. Si, and F. Steglich, Nat. Phys. **4**, 186 (2008).
[3] S. Nakatsuji, D. Pines, and Z. Fisk, Phys. Rev. Lett. **92**, 016401 (2004).
[4] Y.-F. Yang, Z. Fisk, H.-O. Lee, J. D. Thompson, and D. Pines, Nature (London) **454**, 611 (2008).
[5] Y.-F. Yang and D. Pines, Proc. Natl. Acad. Sci. U.S.A. **109**, E3060 (2012).
[6] V. I. Anisimov, M. A. Korotin, M. Zölfl, T. Pruschke, K. Le Hur, and T. M. Rice, Phys. Rev. Lett. **83**, 364 (1999).
[7] R. Arita, K. Held, A. V. Lukoyanov, and V. I. Anisimov, Phys. Rev. Lett. **98**, 166402 (2007).
[8] J. Hopkinson and P. Coleman, Phys. Rev. Lett. **89**, 267201 (2002).
[9] Y. Yamashita and K. Ueda, Phys. Rev. B **67**, 195107 (2003).
[10] J. S. Kim, E. G. Kim, G. R. Stewart, X. H. Chen, and X. F. Wang, Phys. Rev. B **83**, 172502 (2011).
[11] Z. Zhang, A. F. Wang, X. C. Hong, J. Zhang, B. Y. Pan, J. Pan, Y. Xu, X. G. Luo, X. H. Chen, and S. Y. Li, Phys. Rev. B **91**, 024502 (2015).
[12] A. F. Wang *et al.*, Phys. Rev. B **87**, 214509 (2013).
[13] H. Hardy *et al.*, Europhys. Lett. **91**, 47008 (2010).
[14] T. Terashima *et al.*, Phys. Rev. B **87**, 224512 (2013).
[15] T. Sato *et al.*, Phys. Rev. Lett. **103**, 047002 (2009).
[16] K. Haule and G. Kotliar, New J. Phys. **11**, 025021 (2009).
[17] Z. P. Yin, K. Haule, and G. Kotliar, Nat. Mater. **10**, 932 (2011).
[18] F. Eilers *et al.*, arXiv:1510.01857.
[19] P. C. Dai, J. P. Hu, and E. Dagotto, Nat. Phys. **8**, 709 (2012).
[20] F. Hardy *et al.*, Phys. Rev. Lett. **111**, 027002 (2013).
[21] See Supplemental Material at http://link.aps.org/supplemental/10.1103/PhysRevLett.116.147001 for detailed methods of sample growth and experiments, XRD characterization of structure, transport characterization of superconducting transition, bulk magnetization, specific heat, NMR spectrum and detailed analysis of spin-lattice relaxation, which includes Refs. [4–5], [10–12], [30], [22–27].
[22] S. H. Baek, H. -J. Grafe, F. Hammerath, M. Fuchs, C. Rudisch, L. Harnagea, S. Aswartham, S. Wurmehl, J. van den Brink, and B. Büchner, Eur. Phys. J. B **85**, 159 (2012).
[23] V. F. Mitrović, M.-H. Julien, C. de Vaulx, M. Horvatić, C. Berthier, T. Suzuki, and K. Yamada, Phys. Rev. B **78**, 014504 (2008).
[24] J. L. Sarrao, and J. D. Thompson, J. Phys. Soc. Jpn. **76**, 051013 (2007).
[25] C. Pfleiderer *et al.*, Rev. Mod. Phys. **81**, 1551 (2009).
[26] F. F. Tafti, A. Ouellet, A. Juneau-Fecteau, S. Faucher, M. Lapointe-Major, N. Doiron-Leyraud, A. F. Wang, X.-G. Luo, X. H. Chen, and L. Taillefer, Phys. Rev. B **91**, 054511 (2015).
[27] O. Stockert, S. Kirchner, F. Steglich, and Q. Si, J. Phys. Soc. Jpn. **81**, 011001 (2012).
[28] M. Hirano *et al.*, J. Phys. Soc. Jpn. **81**, 054704 (2012).
[29] N. J. Curro, Rep. Prog. Phys. **72**, 026502 (2009).
[30] N. J. Curro, B.-L. Young, J. Schmalian, and D. Pines, Phys. Rev. B **70**, 235117 (2004).
[31] Y.-F. Yang and D. Pines, Phys. Rev. Lett. **100**, 096404 (2008).
[32] K. Ishida, K. Okamoto, Y. Kawasaki, Y. Kitaoka, O. Trovarelli, C. Geibel, and F. Steglich, Phys. Rev. Lett. **89**, 107202 (2002).
[33] Y. Kohori, Y. Yamato, Y. Iwamoto, T. Kohara, E. D. Bauer, M. B. Maple, and J. L. Sarrao, Phys. Rev. B **64**, 134526 (2001).
[34] T. Kohara, Y. Kohori, K. Asayama, Y. Kitaoka, M. B. Maple, and M. S. Torikachvili, Solid State Commun. **59**, 603 (1986).
[35] Y. Mizukami *et al.*, arXiv:1510.02273.
[36] M. Yi *et al.*, Nat. Commun. **6**, 7777 (2015).
[37] D. Pines, J. Phys. Chem. B **117**, 13145 (2013).